Unsupervised seismic facies classification using Independent Component Analysis

David Lubo-Robles and Kurt J. Marfurt, The University of Oklahoma*

Summary

Seismic attributes are powerful tools that allow interpreters to make a more comprehensive and precise seismic interpretation. In this paper, we apply an unsupervised multi-attribute technique called Independent Component Analysis to reduce dimensionality and extract the most valuable information of multiple spectral magnitude components in order to make an unsupervised seismic facies classification of channel complexes located in the Moki A Formation, Taranaki Basin, New Zealand.

Introduction

Depending on the seismic attribute that we choose, different information can be extracted (Infante-Paez and Marfurt, 2017) from the seismic volume, thus, relying on only one attribute information lead to an incomplete seismic interpretation. For this reason, multi-attribute techniques such as Principal Component Analysis (PCA), Self-organizing Maps (SOM) are commonly used.

Based on higher order statistics, Independent Component Analysis separates a multivariate signal into subcomponents which are independent of each other (Hyvärinen and Oja, 2000), thus extracting more valuable information than techniques such as Principal Component Analysis (PCA) which tends to mix geology.

In this research, we use the Tui3D seismic survey located on the Taranaki Basin, New Zealand. The zone of interest is the Moki A Formation which is characterized by base of slope turbidites and channel complexes (Engbers, 2002) trending NW-SE (Yagci, 2016).

Spectral decomposition techniques are commonly used to study the stratigraphy and depositional architecture of a target area (Marfurt and Kirlin, 2001). Thus, using spectral magnitude components as input to Independent Component Analysis and co-rendering independent components that provide the most geological insight, we develop an unsupervised seismic facies classification workflow to better analyze the internal architecture of the channel complexes in the Moki A Formation.

Independent Component Analysis (ICA)

Independent Component Analysis (ICA) separates a multivariate signal into independent subcomponents, finding a linear representation of non-Gaussian data (Hyvärinen and Oja, 2000).

The popular cocktail-party problem is commonly used to illustrate ICA. If two people are speaking simultaneously in a room where two microphones are recording their voices (Figure 1), the recorded signals $\mathbf{X}=\{\mathbf{X_1},\mathbf{X_2}\}$ are a weighted combination of the individual signals spoken by the two people $\mathbf{P}=\{\mathbf{P_1},\mathbf{P_2}\}$, which can be written as:

$$\mathbf{X}=\mathbf{AP}, \quad (1)$$

where $\mathbf{A}$ is an unknown mixing matrix whose parameters depend on the distances between the people and the microphones.

Although the goal is to estimate the original individual signals $\mathbf{P_1}$ and $\mathbf{P_2}$ using the recorded signals $\mathbf{X_1}$ **and** $\mathbf{X_2}$, this cannot be accomplished because the mixing matrix $\mathbf{A}$ is unknown. Nevertheless, Hyvärinen and Oja (2000) stated that under the assumption in which the individual signals are statistically independent, it is possible to compute the inverse of the mixing matrix $\mathbf{A}$ and obtain the independent components $\mathbf{P_1}$ and $\mathbf{P_2}$.

$$\mathbf{P}=\mathbf{WX}, \quad (2)$$

where $\mathbf{W}$ is called the unmixing matrix and is the inverse of the mixing matrix $\mathbf{A}$.

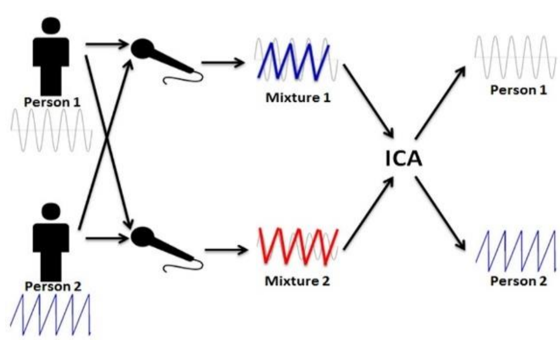

Figure 1. Illustration of ICA using the cocktail-party problem. The objective is to recover the individual signals $\mathbf{P_1}$ and $\mathbf{P_2}$ from the mixed measurements signal components $\mathbf{X_1}$ and $\mathbf{X_2}$.

We modify Hyvärinen and Oja (2000) ICA algorithm for use with volumetric attributes. In our algorithm (Figure 2), first we select the seismic attributes that highlight the geologic feature of interest and compute their means $\boldsymbol{\mu}$ and covariance matrix $\mathbf{C}$ which are used to Z-score normalize the different units of the seismic attributes. We also calculate the eigenvectors and eigenvalues of the covariance matrix $\mathbf{C}$.

To decrease the computational cost of processing several seismic attributes, we decimate the data to construct a smaller training data volume from which the unmixing matrix **W** is computed. The Z-normalized data are whitened and filtered using Principal Component Analysis (Stanford, 2018). The filtering procedure helps to reduce noise, whereby the variance retained exceeding 90% is considered to be signal, while the remaining variability to be noise.

We use a decorrelated version of the covariance matrix **C** as initial guess for the unmixing matrix **W** guaranteeing exact repeatability of the process. Finally, the unmixing matrix **W** is computed by maximizing the non-Guassian behavior of the data measured by an approximation of negentropy (Hyv**ä**rinen and Oja, 2000). When convergence is reached, the Z-normalized and whitened data are projected onto the final unmixing matrix **W** in order to obtain the independent components.

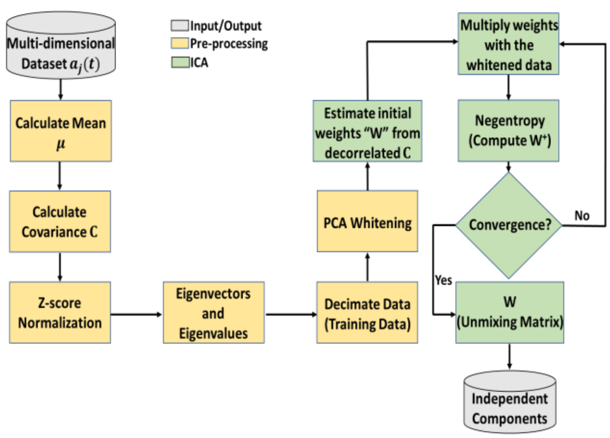

Figure 2. Proposed workflow to apply ICA based on the FastICA algorithm developed by Hyvärinen and Oja (2000) but with modifications in order to implement it using seismic attributes.

Geologic setting

The Taranaki Basin is a sedimentary basin located on the western side of the North Island, New Zealand (Palmer, 1985) (Figure 3) and can be separated into two main structural elements: the eastern Taranaki Graben Complex and the Western Platform (Pilaar and Wakefield, 1984).

The Early to Middle Miocene was characterized by deposition of submarine fans, associated with a major regression. These submarine fans are represented by the Mt Messenger Formation and Moki Formation (De Bock, 1994).

According to Engbers (2002) the Moki Formation can be subdivided from lower to upper units into the Moki B Sands, Moki B Shale and Moki A Sands. The Moki A Sands is the objective of this study and it is represented by base of slope turbidites and major meandering submarine channel complexes (Engbers, 2002) with NW-SE trend (Yagci, 2016).

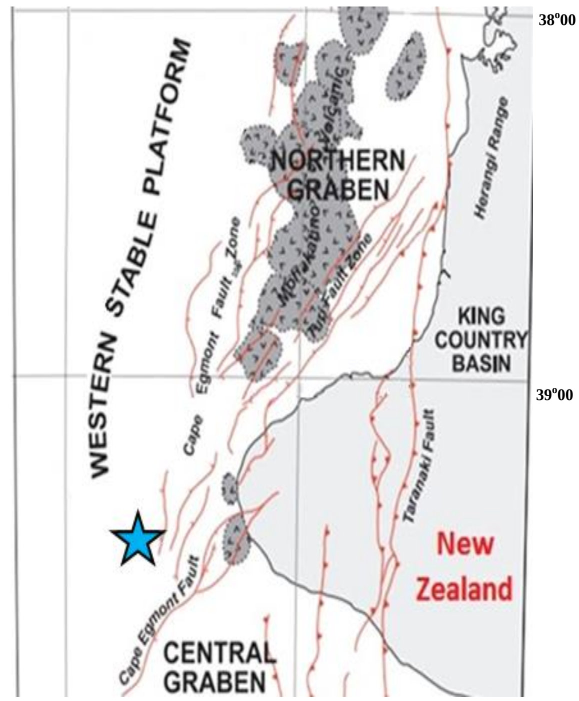

Figure 3. The Tui3D seismic survey (blue star) is situated offshore Taranaki Basin, New Zealand. Following Pilaar and Wakefield, 1984, the Taranaki Basin can be divided in the Taranaki Graben Complex and the Western Platform. After King et. al. (1993), King and Thrasher (1996), Thrasher et. al. (2002) and Hansen and Kamp (2006).

Data description

The Tui3D seismic survey is located offshore Taranaki Basin on the southwest coast of the North Island, New Zealand (Figure 3). For this study, the seismic volume was cropped consisting of 821 inlines and 2001 crosslines with bin size of 12.5 by 12.5 m. The Tui3D seismic volume is contaminated by acquisition footprint.

To study the internal facies architecture and highlight the channel complexes present in the Moki A Formation, we use a total of twelve spectral magnitude components ranging from 25 to 80 Hz at 5 Hz interval computed using a Continuous Wavelet Transform (CWT) Spectral Decomposition technique (Sinha et. al., 2005; Chopra and Marfurt, 2016). CWT spectral decomposition provides good vertical resolution allowing us to study changes in bed-thickness and the stratigraphy and depositional system of the Moki A Formation.

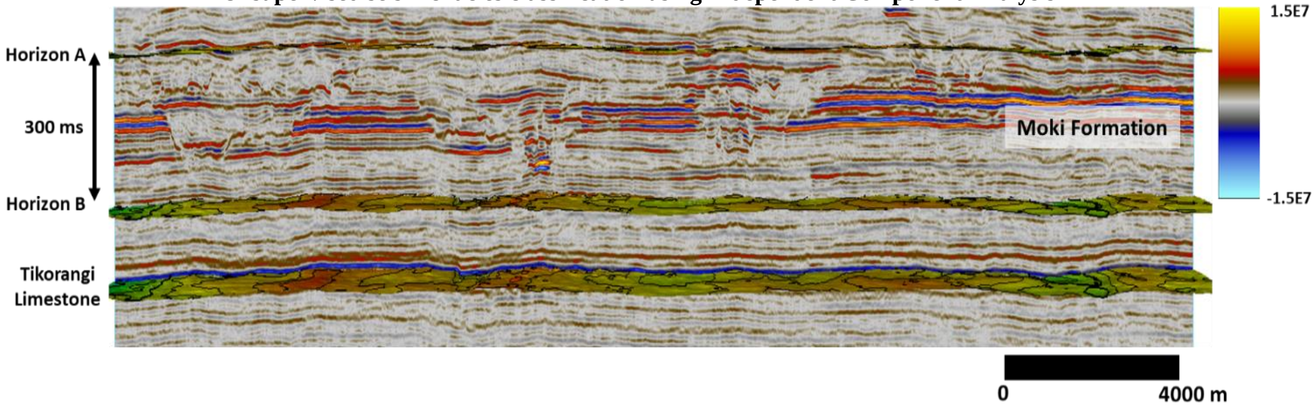

Figure 4. Analysis interval between Horizon A and Horizon B enclosing the Moki Formation. A strong continuous reflector associated with the Tikorangi Limestone was picked and phantom horizons were created bracketing the Moki Formation. The analysis interval has a width of 300 ms.

To design our analysis interval, we picked a horizon along a strong continuous reflector associated with the Tikorangi Limestone and created phantom horizons on top and base of the Moki Formation (Figure 4). Even though the ideal analysis interval to make a unsupervised facies analysis consist on enclosing only one target formation, in our case in order to completely enclose the channel complexes, our analysis interval brackets the Moki A Formation, the Moki B Shale and part Moki B Sands Formation.

Unsupervised facies analysis using ICA

We use twelve spectral magnitude components ranging from 25 to 80 Hz as input in the Independent Component Analysis algorithm. The independent components extract the most important information, thus reducing dimensionality and noise. Based on the retained variability criteria (Stanford, 2018), our algorithm automatically outputs four independent components because they represent 94.04% of the variability of the data.

In Figure 5 we show the four independent components extracted along a phantom Horizon A + 208 ms. In addition, the independent components are sorted by visual inspection because during their computation the order of the independent component is undefined (Hyvärinen and Oja, 2000).

Analyzing independent component 1 (IC1) at Horizon A+208 ms in Figure 5a, we note the presence of two meandering channels with moderate sinuosity and a tubular shape channel with an architecture similar to a braided channel (green arrows). Even though there is acquisition footprint (red rectangle), the picture looks smoother, exhibiting both large scale and small scale geological features such as an abandoned channel (blue arrow) and oxbows (orange arrows). In Figure 5b, we display independent component 2 (IC2) at Horizon A + 208 which also exhibits the large and small scale geological features. Although there is a slight increase in the acquisition footprint (red rectangle) compare to IC1, the image still has good lateral resolution and provides geological insight.

From Figure 5c, we observe that the independent component 3 (IC3) is characterized by an increase in the acquisition footprint (red rectangle) and random noise. The large scale channel complexes (green arrows) and the oxbows (orange arrows) are still resolved, but the small abandoned channel (blue arrow) is no longer seen using IC3. Finally, the independent component 4 (IC4) (Figure 5d) is associated with strong acquisition footprint (red rectangle) and random noise. Large and small scale geological features are difficult to interpret, thus we consider that IC4 does not provide valuable geological insight.

Because the spectral magnitude components are reduced to a 4D space represented by the independent components, in which the data is whitened and then projected onto the unmixing matrix **W**, if we plot the independent components against an RGB color scheme, voxels that project to similar colors can be associated with similar seismic facies.

In Figure 6, we show a RGB blending using the IC1, IC2 and IC3 at Horizon A + 208 ms. We observe that the large scale features such as the meandering channels and the tabular shape channel (green arrows) and the small scale geological features such as oxbows (orange arrows) and the small abandoned channel (blue arrow) are well preserved. We also note a strong contrast of seismic facies between the axis and the flank of the meandering channels, i.e., the former are associated with a purple seismic facies, while the latter are characterized by a green seismic facies. On contrast, the tabular shape with braided architecture channel is characterized by a predominant purple seismic facies with some intercalations of green and blue seismic facies. The small abandoned channel is also associated with purple seismic facies. The oxbows infill vary from purple to green and blue seismic facies.

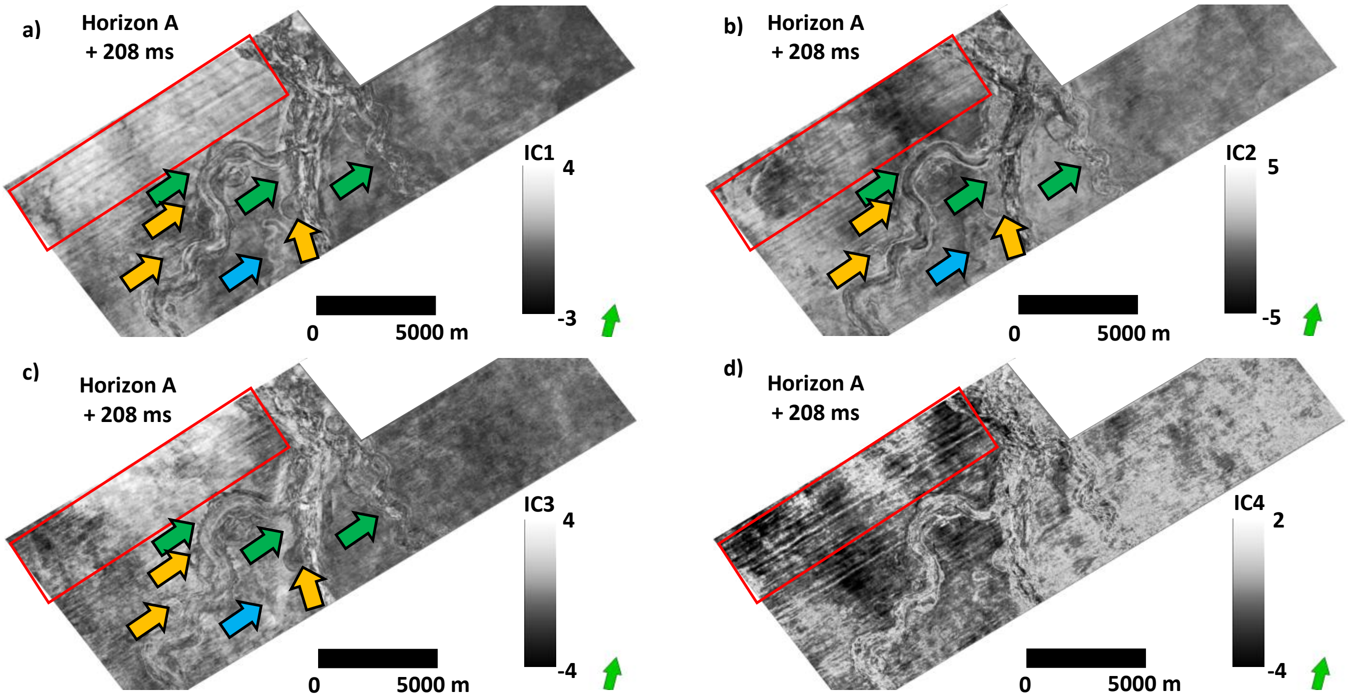

Figure 5. (a) Independent Component 1 showing two meandering channels and a tabular shape channel (green arrows) together with oxbows (orange arrows) and a small abandoned channel (blue arrow). Footprint is seen (red rectangle) but geologic features are well resolved. (b) Independent component 2. Large scale (green arrows) and small scale (blue and orange arrows) features are well delineated. Acquisition footprint (red rectangle) increases compared to IC1. (c) Independent component 3 characterized by an increase in random noise and acquisition footprint (red rectangle). Geological features (green and orange arrows) except the small abandoned channel (blue arrow) are interpretable. (d) Independent component 4 characterized by strong footprint (red rectangle) and random noise with little geological insight. All independent components are extracted along a phantom Horizon A + 208 ms.

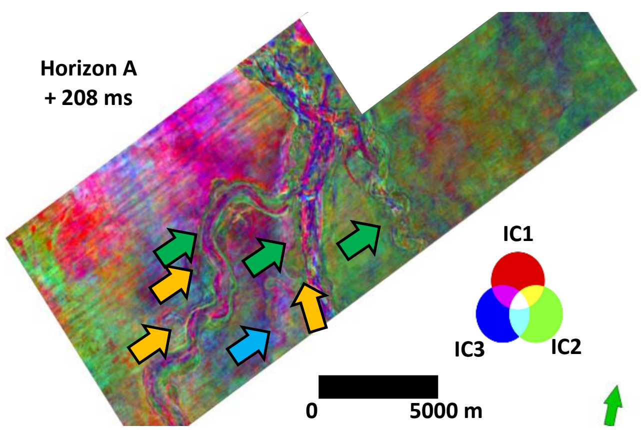

Figure 6. Voxels projected to similar colors, represent similar seismic facies. The axis of the meandering channels is represented by purple seismic facies, while their flanks are characterized by green seismic facies. The tabular shape channel is associated with purple seismic facies with some green and blue facies. Finally the small abandoned channel (blue arrow) is characterized by purple seismic facies and the oxbow (orange arrows) infill vary from purple to blue and green seismic facies.

Conclusions and future work

Independent Components Analysis (ICA) proved to be a powerful technique to reduce dimensionality, reduce noise and extract valuable information from multiple seismic attributes. Also, projecting the independent components against a RGB color scheme it is possible to make an unsupervised seismic facies classification. For future work, we will relate the seismic facies with axial and off-axis deposition in deepwater channels and compare the results obtained using ICA to the results using Principal Component Analysis (PCA).

Acknowledgements

We thank New Zealand Petroleum and Minerals for providing the Tui3D seismic data to the public for use in research and education. Also, we would like to thank the sponsors of the Attribute Assisted Seismic Processing and Interpretation (AASPI) consortium for their support. We also thank Schlumberger for the licenses in Petrel, provided to the University of Oklahoma and Lennon Infante, Richard Brito, Thang Ha and Emilio Torres for their valuable comments.

Unsupervised seismic facies classification using Independent Component Analysis

References

Chopra, S., Marfurt, K. J., 2016, Spectral decomposition and spectral balancing of seismic data: The Leading Edge, 35, 176-179, doi: 10.1190/tle35020176.1.

De Bock, J.F., 1994, Moki Formation, a Miocene reservoir sequence, its facies distribution and source in offshore southern Taranaki Basin: New Zealand Petroleum Conference Proceedings, 155-167.

Engbers, P., 2002, Evaluation of Moki sands prospectivity in Maui PML: New Zealand Petroleum Conference Proceedings, Ministry of Economic Development.

Hansen, R. J., and P. J. Kamp, 2006, An integrated biostratigraphy and seismic stratigraphy for the late Neogene continental margin succession in northern Taranaki Basin, New Zealand: New Zealand Journal of Geology and Geophysics, 49, no. 1, 39–56.

Hyvärinen, A., and E. Oja, 2000, Independent Component Analysis: Algorithms and Applications: Neural Networks, **13,** nos. 4-5, 411-430.

Infante-Paez, L., and K. Marfurt, 2017, Seismic expression and geomorphology of igneous bodies: A Taranaki Basin, New Zealand, case study: Interpretation, **5**, no. 3, 121-140.

King, P. R., G. H. Scott, and P. H. Robinson, 1993, Description, correlation and depositional history of Miocene sediments outcropping along North Taranaki coast: Institute of Geological & Nuclear Sciences Ltd., p. 199.

King, P. R., and G. P. Thrasher, 1996, Cretaceous Cenozoic geology and petroleum systems of the Taranaki Basin, New Zealand: Institute of Geological & Nuclear Sciences 2.

Marfurt, K. J., and R.L. Kirlin, 2001, Narrow-band spectral analysis and thin-bed tuning: Geophysics, **66**, 1274–1283.

Palmer, J, 1985, Pre-Miocene lithostratigraphy of Taranaki Basin, New Zealand: New Zealand Journal of Geology and Geophysics, **28**, no. 2,197-216.

Pilaar, W.F.H, and L.L. Wakefield, 1984, Hydrocarbon generation in the Taranaki Basin, New Zealand: AAPG Special Volumes M35, Petroleum Geochemistry and Basin Evaluation, 405-423.

Sinha S., P. Routh, P. Anno, and J. Castagna, 2005, Spectral decomposition of seismic data with continuous-wavelet transform: Geophysics, **70**, no. 6, 19-25.

Stanford, 2018, PCA Whitening: http://ufldl.stanford.edu/tutorial/unsupervised/PCAWhitening/. Accessed on March 26th, 2018.

Thrasher, G. P., B. Leitner, and A. W. Hart, 2002, Petroleum system of the Northern Taranaki Graben: New Zealand Petroleum Conference Proceedings, Ministry of Economic Development.

Yagci, G., 2016, 3D seismic structural and stratigraphic interpretation of the Tui-3D field, Taranaki Basin, New Zealand: Master's Thesis, Missouri University of Science and Technology.